3 Biotech (2019) 9:221
https://doi.org/10.1007/s13205-019-1748-y

ORIGINAL ARTICLE

Characterization of biogenic selenium nanoparticles derived from cell-free extracts of a novel yeast *Magnusiomyces ingens*

Shengyang Lian[1] · Catherine Sekyerebea Diko[1] · Yongquan Yan[1] · Zheng Li[1] · Henglin Zhang[1] · Qiao Ma[2] · Yuanyuan Qu[1]

Received: 30 January 2019 / Accepted: 8 May 2019 / Published online: 20 May 2019

Abstract

A facile one-pot and effective green process for biogenic selenium nanoparticles (SeNPs) was obtained using the cell-free extracts of a novel yeast *Magnusiomyces ingens* LH-F1. The corresponding absorption peak of SeNPs was observed at ~ 560 nm by UV–vis spectrophotometer. In the present study, SeO_2 2 mM, protein 500 mg L^{-1} and pH 7 were preferable to the biosynthesis of SeNPs. The effects of pH, SeO_2 concentration and protein concentration on the synthesis process were different. Transmission electron microscopy image exhibited that all the SeNPs were spherical and quasi-spherical with the diameters mainly distributed in 70–90 nm (average particles size was 87.82 ± 2.71 nm). X-ray diffraction suggested that the nanoparticles were composed of standard hexagonal crystalline Se with high purity. Fourier transform infrared spectroscopy indicated that some biomolecules such as hydroxyl, carboxyl and amino groups in the yeast cell-free extracts might be involved in the formation of SeNPs. Analyses of sodium dodecyl sulfate–polyacrylamide gel electrophoresis revealed that two proteins with low molecular weight approximately ~ 16 and ~ 21 kDa were detected on the surface of SeNPs and in the extracts, which could play the role of natural stabilizers and confer stability to synthesized SeNPs; whereas, unbound proteins on the SeNPs surface could act as reducing agents. Antibacterial analysis showed that the SeNPs could inhibit *Arthrobacter* sp. W1 (Gram positive) but not *E. coli* BL21 (Gram negative), which could provide reference for antimicrobial application of biogenic SeNPs.

Keywords Selenium nanoparticle · Biosynthesis · *Magnusiomyces ingens* · Antibacterial activity

Introduction

Selenium (Se) is a key microelement for creatures, which is closely related to a series of major metabolic pathways such as anti-oxidant systems, thyroid hormone metabolism, growth modulation and immune function (Stranges et al. 2006; Kumar et al. 2018; Xia et al. 2018). It has also been reported that Se deficiency (< 40 μg/day) can lead to many diseases, while excessive intake will cause Se poisoning (> 400 μg/day) (Gore et al. 2010; Vogel et al. 2018). In natural environments, Se is unevenly distributed in the aquatic, terrestrial and atmospheric compartments, which often exists in one or more of the four oxidation states, i.e., selenate (Se-VI); selenite (Se-IV); selenium elemental (Se-0) and selenide (Se-II) (Gore et al. 2010). Selenite (Se-IV) is soluble and highly toxic toward biota, while Se-0 is insoluble with low toxicity (Lampis et al. 2017; Xia et al. 2018). From the above mentioned, it seems to be beneficial for the ecological environment and human beings to convert Se-IV into element Se-0.

Recently, the conversion of inorganic ions into inorganic nanoparticles using microorganism (viruses, bacteria, yeast and fungi either in intracellular or extracellular) has become a matter of great concern owing to its

Electronic supplementary material The online version of this article (https://doi.org/10.1007/s13205-019-1748-y) contains supplementary material, which is available to authorized users.

✉ Yuanyuan Qu
qyy@dlut.edu.cn

[1] State Key Laboratory of Fine Chemicals, Key Laboratory of Industrial Ecology and Environmental Engineering (Ministry of Education), School of Environmental Science and Technology, Dalian University of Technology, Dalian 116024, People's Republic of China

[2] Institute of Environmental Systems Biology, College of Environmental Science and Engineering, Dalian Maritime University, Dalian 116026, People's Republic of China

advantages of environmental friendliness and cost effective (Park et al. 2016; Singh et al. 2016). Many researches have indicated that bacteria can form zero-valent Se particles under aerobic or anaerobic conditions (e.g. *Veillonella atypical, Geobacter sulfurreducens, Bacillus cereus, Agrobacterium* sp., *Bacillus subtilis, Shewanella putrefaciens, Stenotrophomonas maltophilia, Pseudomonas aeruginosa*) (Vogel et al. 2018). Various types of biomolecules may serve as reducing agents and stabilizers in the formation of inorganic nanoparticles (Moghaddam et al. 2015). Therefore, microorganisms can produce the nanoparticles with good bio-compatibility and dispersion without additional chemical reagents.

Selenium nanoparticles (SeNPs) have excellent photoelectric, semiconductor properties, physical and chemical properties, which make them unique from bulk materials (Zhang et al. 2004; Tugarova and Kamnev 2017). Not only have SeNPs been widely used in solar cells, rectifiers, sensors and other optoelectronic components, but also they have shown great potential applications in various fields of biotechnology, medicine and environmental remediation (Zhang et al. 2004; Dykman and Khlebtsov 2012; Chaudhary et al. 2014; Schröfel et al. 2014; Khiralla and El-Deeb 2015; Kumar et al. 2015; Sonkusre and Singh Cameotra 2015; Eswayah et al. 2016; Vera et al. 2016). The biosynthesis of SeNPs by living microorganisms is widely distributed in nature, which has drawn attentions over the last 10 years (Wadhwani et al. 2016; Lampis et al. 2017; Tugarova and Kamnev 2017). From one point of view, SeNPs formed by biological sources possess momentous antimicrobial activity to pathogenic fungi, yeast and bacteria (Fernández-Llamosas et al. 2016). However, few reports have described fungal mediation up to now (Wadhwani et al. 2016). Meanwhile, researches have already speculated the mechanism of the SeNPs formation in the bacteria through strain *Thauera selenatis* (Butler et al. 2012), but the universal biochemical and molecular mechanism of reducing Se-IV to element Se-0 in the fungus is still unknown. Therefore, it is necessary for us to explore the SeNPs synthesis ability of novel yeast LH-F1 isolated from marine mud (Tan et al. 2014; Zhang et al. 2016) and the application of as-synthesized SeNPs.

In this study, the Selenium dioxide (SeO_2) concentration, initial pH and cell-free extracts (proteins) concentration of SeNPs biosynthesis were discussed in details. Then, the SeNPs were characterized by transmission electron microscopy (TEM), X-ray diffraction (XRD) and UV–vis spectroscopy. Sodium dodecyl sulfate–polyacrylamide gel electrophoresis (SDS-PAGE) and Fourier transform infrared (FTIR) spectroscopy were used to further explore the biosynthesis mechanism of SeNPs. *E. coli* BL21 (Gram negative) and *Arthrobacter* sp. W1 (Gram positive) were used to investigate the antibacterial property of the biosynthesized SeNPs.

Materials and methods

Materials

SeO_2 was obtained from Chinese Sinopharm Chemical Regent Beijing Co., Ltd. Other chemical reagents were analytically pure.

The yeast LH-F1 (CGMCC No. 10367) was previously isolated and purified from the marine mud of Dalian in China, which was routinely cultivated with the modified martin medium (1.0 g L^{-1} NH_4SO_4, 1.0 g L^{-1} glucose, 0.5 g L^{-1} $MgSO_4{\cdot}7H_2O$ and 1.0 g L^{-1} KH_2PO_4) (Tan et al. 2014; Zhang et al. 2016).

Biosynthesis of SeNPs by yeast LH-F1 cell-free extracts

One milliliter of yeast LH-F1 at the end of logarithmic growth was added to 99-mL cultivation medium with continuous shaking for 24 h (30 °C) under aerobic condition. Yeast LH-F1 cells were collected through centrifuge (12,000*g*, 10 min, 4 °C), washed three times with 50-mM phosphate buffer saline (PBS), and resuspended with PBS. The resuspended yeast LH-F1 cell was broken by ultrasound (Ultrasonic Processor CPX 750, USA) for 60 min. The cell lysate was centrifuged (12,000*g*, 30 min) and then filtered through syringe Millipore filter (pore size: 0.45 μm, inner filtration membrane: PES, dia.: φ 13 mm) to obtain the cell-free extracts. The concentration of protein was tested by Bradford assays, which was used to indicate the concentration of yeast LH-F1 cell-free extracts (Qu et al. 2018). To biosynthesize SeNPs, 2-mM SeO_2 was added to the 300 mg L^{-1} of protein (pH 7), and then the reaction was carried out under sustained shaking (30 °C) until a plateau was reached.

The influence of initial Se ion concentration on SeNPs synthesis was investigated using different concentrations of SeO_2 with 0.5, 1.0, 2.0, 3.0 and 5.0 mM. As for the pH effects, the pH of PBS was adjusted to 5, 6, 7, 8 and 9. To investigate the effects of protein concentration on SeNPs synthesis, protein with different concentrations of 100, 200, 300, 400 and 500 mg L^{-1} was prepared.

Characterization

SeNPs were characterized by several methods. The synthesis of SeNPs was demonstrated using Metash UV-9000 UV–vis spectrophotometer (Shanghai, China). TEM (FEI Tecnai G220 S-Twin, USA) was used to investigate the morphology and distribution of SeNPs. The D/max-2400 diffractometer (Rigaku, Japan) was used to analyze the crystalline structure. FTIR spectra of SeNPs and yeast LH-F1 cell-free extracts

were obtained using a FTIR spectrophotometer (Shimadzu IRPrestige-21, Japan). The inductively coupled plasma optical emission spectrometer (ICP-OES, Perkin-Elmer Optima 2000 DV, USA) was applied to measure the concentration of SeNPs.

SDS-PAGE analysis

SDS-PAGE was performed to assess the protein associated with the formation of SeNPs. The modified methods of the experiment were carried out according to Das et al. (2012). Briefly, SeNPs were synthesized by cell-free extracts, the unbound proteins were removed by centrifugation at 14,000*g* for 20 min, and then washed three times with sterile ultrapure water before resuspended in sterile ultrapure water. The resuspended SeNPs and original yeast LH-F1 cell-free extracts would be used for SDS-PAGE analysis. Perform SDS-PAGE experiment with acrylamide gels (12%) as described by Laemmli (1970).

Antibacterial analysis of SeNPs

The antibacterial activity of SeNPs was performed using the modified disc method (Jayaramudu et al. 2013, 2017). First, Luria-Bertani (LB) medium was prepared by mixing 10 g of sodium chloride, 10 g of peptone and 5 g of yeast extract powder in 1 L ultrapure water, then the pH of the medium was adjusted to 7. The last step was to mix 20 g of agar with the medium. The prepared agar medium was sterilized by autoclave (121 °C, 20 min) and poured into germfree glass petri dishes at room temperature. Furthermore, when the agar media solidified, 200 µL of *E. coli* BL21 (Gram negative) and 200 µL of *Arthrobacter* sp. W1 (a Gram-positive bacterium that can reduce phenol hydrolysis in high-salt environment previously screened by our laboratory) were spread on the surface of the media, respectively. Finally, different volumes (10 µL, 20 µL) of the SeNPs solution (6.232 mg L^{-1}) were added to the inoculated glass petri dishes, and cultivated for 24 h at 37 °C with sterilized ultrapure water and PBS as control. During this period, the growth of bacterial colonies was observed and recorded.

Results and discussion

Effects of SeO_2 concentration on SeNPs biosynthesis

Different concentrations of SeO_2 (0.5–5 mM) were used to study the effects of SeO_2 concentrations on SeNPs biosynthesis. UV–vis spectra showed a characteristic absorption peak at around 560 nm, due to the surface plasmon resonance (SPR) of SeNPs (Fig. 1, Table S1). The intensity of SPR peak increased with the incubation time, which was

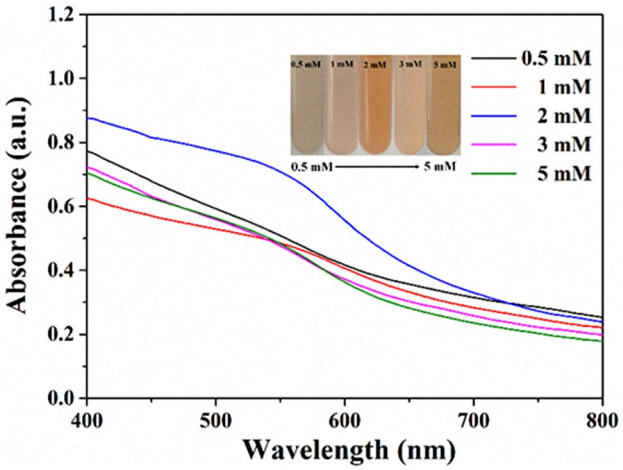

Fig. 1 UV–vis spectra of stable SeNPs under different SeO_2 concentrations (mM): 0.5 (84 h), 1 (120 h), 2 (132 h), 3 (132 h), 5 (96 h). The illustration exhibited the solution color at different SeO_2 concentrations

depending on the SeNP concentrations (Table S1) (Gates et al. 2002; Lin and Wang 2005; Qu et al. 2018). The stabilization time of SeNPs synthesis was 84 h (0.5 mM), 120 h (1 mM), 132 h (2 mM), 132 h (3 mM) and 96 h (5 mM), respectively. With the SeO_2 concentration increasing, the intensity of SPR peak tended to be stronger (0.5–2 mM) and then to be weaker (2–5 mM). Meanwhile, the solution color changed gradually with the incubation time, and the darkest color was obtained with 2-mM SeO_2. The above-mentioned phenomenon could be related to the relative concentrations of the biomolecules and precursor in the reaction solution, which affected the processes of the selenium ions (Se-IV) reduction and Se-0 capping further (Lin and Wang 2005; Zhang et al. 2010). First, Se-IV was reduced to unstable Se-0 using cell-free extracts. And then some biomolecules could stabilize the Se nanocrystals and prevent the agglomeration of SeNPs (Lin and Wang 2005; Debieux et al. 2011). Therefore, it was possible to speculate that the amount of SeNPs synthesis decreased with the relatively high or low SeO_2 concentration; thus, 2-mM SeO_2 was considered as the optimal concentration in the present study. In summary, it could be inferred that SeO_2 concentration had a significant effect on the formation of SeNPs.

Effects of protein concentration on SeNPs biosynthesis

To research the effects of protein concentration on SeNPs biosynthesis, yeast LH-F1 cell-free extracts with different initial protein concentration (100–500 mg L^{-1}) were used in the experiment. As shown in Fig. 2 and Table S2, as the protein concentration raised, the intensity of SeNPs SPR peak increased, and the color changed from yellowish

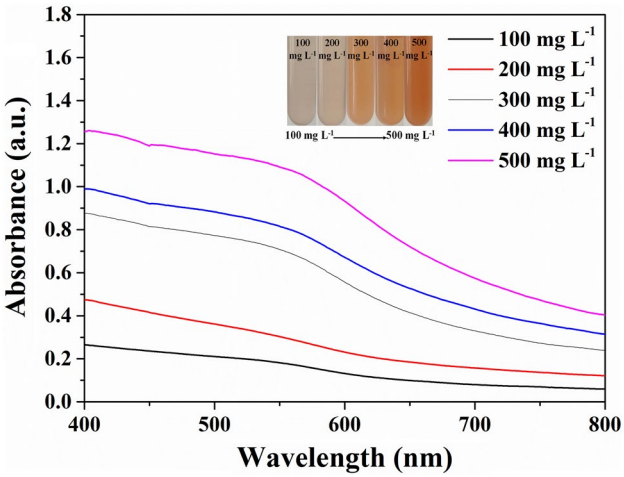

Fig. 2 UV–vis spectra of stable SeNPs under different protein concentrations (mg L^{-1}): 100 (120 h), 200 (96 h), 300 (132 h), 400 (132 h), 500 (108 h). The illustration exhibited the solution color at different protein concentrations

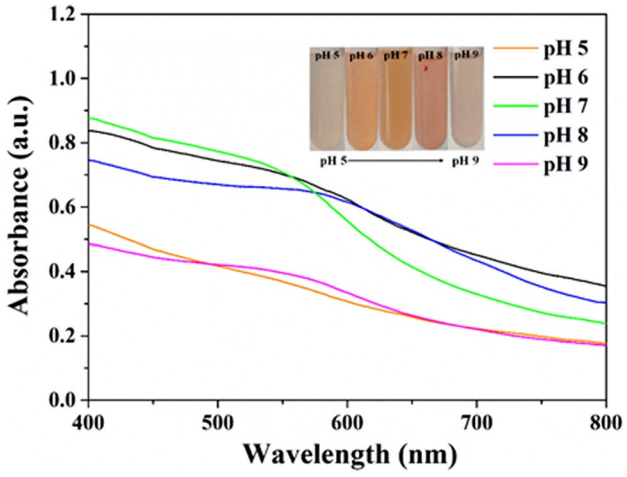

Fig. 3 UV–vis spectra of stable SeNPs under different pH: 5 (132 h), 6 (132 h), 7 (132 h), 8 (132 h), 9 (120 h). The illustration exhibited the solution color at different pHs

orange to deep red, indicating that the amount of SeNPs increased. Meanwhile, the stabilization time of SeNPs synthesis became shorter (120–96 h), since the initial protein concentrations changed from 100 to 200 mg L^{-1}. Similarly, as the initial protein concentrations continued increasing (300–500 mg L^{-1}), the stabilization time of SeNPs synthesis changed from 132 to 108 h (Table S2). The changes of SeNPs stabilization time could be related to the process of reduction and stabilization of Se-IV, which followed a sequential series of redox step ultimately leading to the synthesis of SeNPs (Debieux et al. 2011). Butler et al. (2012) suggested that bacterial protein could function as stabilizing agents of SeNPs, which possibly provided reaction sites for SeNPs biosynthesis or a shell to prevent subsequent SeNPs aggregation (Butler et al. 2012). Due to low protein concentration, it could be surmised that the reducing agents were not enough to reduce more Se-IV to the final step and the capping agents were relatively sufficient, leading to accelerating of stabilization time. However, as the protein concentration gradually increased, the reducing agents were enough to reduce more Se-IV to SeNPs, making the stabilization time of SeNPs synthesis get longer. Dobias et al. (2011) revealed that bacterial protein might become an important tool in the formation of SeNPs (Dobias et al. 2011). Similarly, the present study indicated that protein concentration could distinctly influence both formation and stabilization processes of SeNPs.

Effects of pH on SeNPs biosynthesis

The relationship between SeNPs biosynthesis and initial pH was examined through the change of UV–vis spectra and solution color. As shown in Table S3 and Fig. 3, the SPR peak intensity and color depth of solution had obvious change with different pH (5–9). With low pH (5) or high pH (9), the solution had light color with weak SPR peaks. Among these different experiment groups, the SPR peak intensity was the highest when pH was 7. In UV–vis spectra, most of the corresponding SPR peaks of SeNPs were at about 560 nm with undetected difference, and the solution colors were yellowish orange (Table S3 and Fig. 3). However, when pH was 8, the corresponding peak had a significant red shift from 560 to 580 nm, and solution color turned to dark red, which could be directly attributed to the formation of big-size particles (Lin and Wang 2005). Besides, while the initial solution pH changed from 5 to 9, the stabilization time of SeNPs synthesis were all almost 132 h except for 120 h at pH 9. It could be inferred that pH had a relatively small effect on the stabilization time of selenium synthesis. Che et al. (2017) revealed that bacterium *Lysinibacillus* sp. ZYM-1 could reduce Se-IV to Se nanomaterials at pH from 5 to 9, and the optimal pH was 7, which was similar to our results (Che et al. 2017).

Characterization of SeNPs

The TEM image showed that the SeNPs were almost quasi-spherical and spherical with a good size distribution, while a small number of irregular SeNPs had also been obtained (Fig. 4). From TEM image, the edge length of the biogenic SeNPs ranged from 8.12 to 198.85 nm. The diameter was mainly distributed in 70–90 nm (the average particles size was 87.82 ± 2.71 nm). Shakibaie et al. (2010) demonstrated that most of SeNPs synthesized by bacteria isolated from the

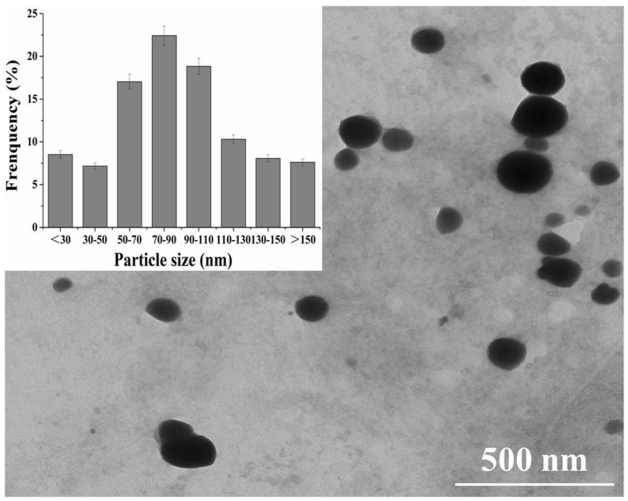

Fig. 4 TEM image of SeNPs. The insert exhibited particle size distribution histograms

sea were 80–220 nm in diameter, which was a bigger range than our results (Shakibaie et al. 2010).

A typical XRD pattern of SeNPs is displayed in Fig. 5. Eleven prominent peaks were obtained at 2θ values of 71.54°, 65.21°, 61.62°, 55.94°, 51.56°, 47.84°, 45.20°, 43.50°, 41.14°, 29.52° and 23.12°, corresponding to (113), (210), (202), (112), (201), (200), (111), (102), (110), (101) and (100) planes of the standard hexagonal phase of crystalline Se with average grain size of 13.7 nm (JCPDS No. 06-0362). The lattice constants were calculated as a (4.3745 Å) and c (4.95452 Å) (JCPDS No. 06-0362), which was corresponded to the hexagonal phase selenium ($a = 4.366$ Å, $c = 4.9536$ Å) (Srivastava and Mukhopadhyay 2013). The peak signal corresponding to (101) plane was

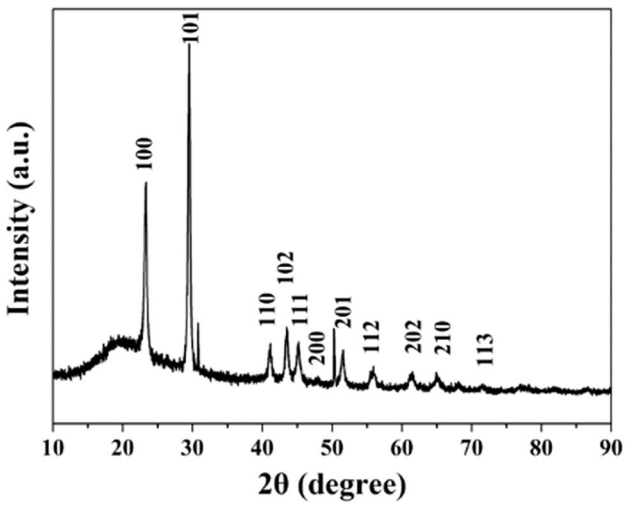

Fig. 5 XRD analysis of SeNPs

stronger than the others, suggesting that (101) plane was the primary orientation. The results revealed that the synthesized SeNPs were composed of crystalline Se with high purity.

The functional groups in the yeast LH-F1 cell-free extracts might be responsible for the reduction of SeO_2 to Se-0 and act as stabilizer to prevent biosynthesized SeNPs aggregation. From Fig. 6, the FTIR spectrum of SeNPs was very similar to the one of yeast LH-F1 cell-free extracts,

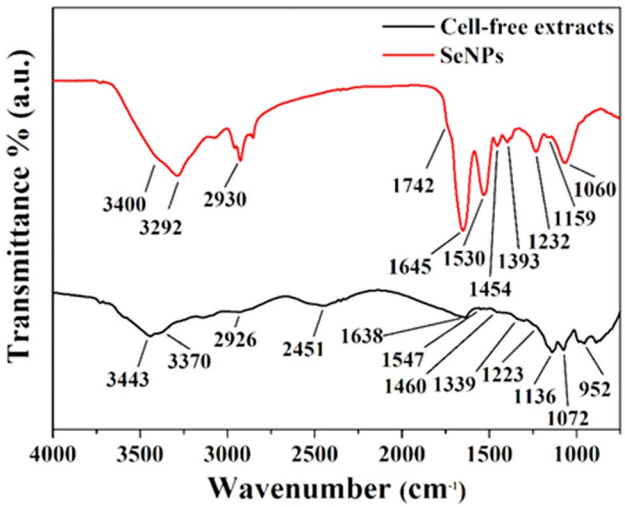

Fig. 6 FTIR analysis of SeNPs and yeast LH-F1 cell-free extracts

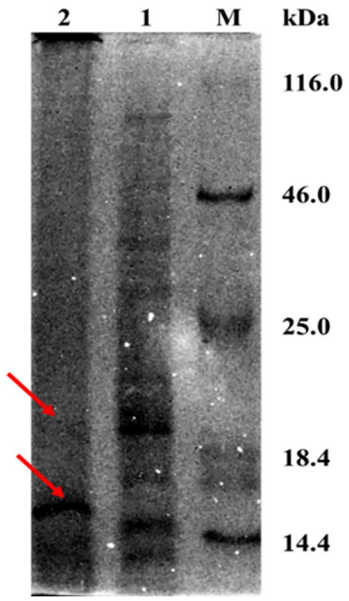

Fig. 7 SDS-PAGE analysis of SeNPs and yeast LH-F1 cell-free extracts. Lane 2, bound proteins absorbed on SeNPs; lane 1, proteins of yeast LH-F1 cell-free extracts; lane M, standard protein molecular weight marker. Arrows indicated ~ 16 and ~ 21 kDa proteins

showing absorption bands at ~ 3400, ~ 3300, ~ 2930, ~ 1650, ~ 1540, ~ 1450, ~ 1390, ~ 1230, ~ 1150 and ~ 1070 cm^{-1}. The bands at ~ 3400 cm^{-1} and ~ 3300 cm^{-1} were owed to the amide (–NH) groups or hydroxide (–OH) stretching vibration (Mishra et al. 2011; Zhang et al. 2016). The band at ~ 2930 cm^{-1} was the characteristic of stretching vibration of saturated aliphatic group (Ahmed et al. 2014). The weaker peaks at ~ 1740 cm^{-1} and ~ 1450 cm^{-1} were probably related to carboxyl groups (–COOH) (Ahmed et al. 2014; Tugarova et al. 2018). The bands at ~ 1450 cm^{-1}, ~ 1540 cm^{-1} and ~ 1650 cm^{-1} should be related to amide III, amide II and amide I, respectively (Tugarova et al. 2018; Xia et al. 2018). The peaks appeared in finger print region (1200–900 cm^{-1}) were probably corresponding to stretching vibration of C–OH or C–O–C groups (Ahmed et al. 2014; Shen et al. 2017). In addition, the peaks at ~ 2450 cm^{-1} and ~ 950 cm^{-1} did not appear in the FTIR spectra of SeNPs, but a new peak at ~ 1740 cm^{-1} appeared; it was speculated that some triple bands or double bonds in the yeast LH-F1 cell-free extracts were involved in the forming of SeNPs, and –COOH or –COOR might be the oxidation products. FTIR data indicated that hydroxyl, carboxyl groups and amine might play a significant role in the SeNPs synthesis process. Tugarova et al. (2018) reported that polysaccharides and proteins in the biomacromolecules were coated on the SeNPs surface (Tugarova et al. 2018). Xia et al. (2018) demonstrated that SeNPs might contain organic substances, some lipids, proteins and inorganic ions, which act as stabilizing agents to stabilize SeNPs (Xia et al. 2018). These reports were consistent with our analysis results.

The results of SDS-PAGE showed that some protein bands were predominantly observed in yeast LH-F1 cell-free extracts (Fig. 7, lane 1), but only two proteins with low molecular weight approximately ~ 16 and ~ 21 kDa were bounded on the surface of SeNPs (Fig. 7, lane 2). The proteins detected on SeNPs were also presented in extracts, which could play the role of natural stabilizers and confer stability to synthesize SeNPs, while unbound proteins on the SeNPs surface could act as reducing agents (Fig. 7) (Das et al. 2012; Tugarova and Kamnev 2017). Malhotra et al. (2013) reported that certain small proteins were likely to play a significant role in the formation of metal nanoparticles, and eventually converting them into nano-structure should be attributed to their presence or absence (Malhotra

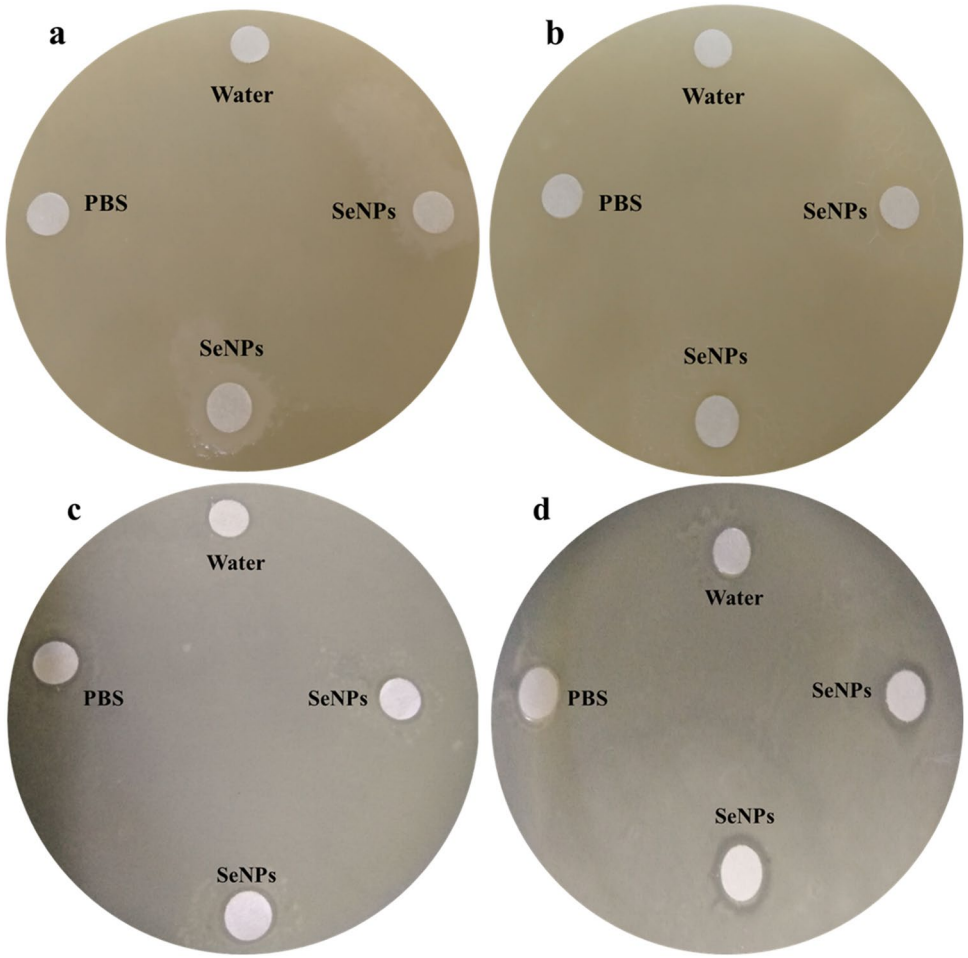

Fig. 8 Antibacterial activity of: **a** water (10 µL), PBS (10 µL) and SeNPs (10 µL); **b** water (20 µL), PBS (20 µL) and SeNPs (20 µL) on *E. coli* BL21 and **c** water (10 µL), PBS (10 µL) and SeNPs (10 µL); **d** water (20 µL), PBS (20 µL) and SeNPs (20 µL) on *Arthrobacter* sp. W1

et al. 2013). Thus, it could be proposed that a variety of proteins from the surface of SeNPs were associated with the reduction and stabilization of SeNPs. However, the specific mechanism was not yet clear, and further studies were needed to understand the actual underlying mechanism of the metal nanoparticles synthesis.

Antibacterial activity

The antibacterial properties of SeNPs synthesized using yeast LH-F1 cell-free extracts were investigated on agar medium by detecting their ability of inhibiting the growth of Gram-positive bacteria *Arthrobacter* sp. W1 and Gram-negative bacteria *E. coli* BL21. After 24-h incubation, results showed that inhibition zone of SeNPs was only found in *Arthrobacter* sp. W1 (Fig. 8c and d). The diameters of antibacterial region were 0.05 mm and 1.2 mm by adding 10 uL and 20 uL SeNPs, respectively. According to previous literatures and the Standard Antibacterial methods (SNV 195920-1992), samples exhibiting more than 1-mm microbial inhibition zone can be considered to have a good antibacterial effect (Raghavendra et al. 2013; Jayaramudu et al. 2017). Therefore, the biosynthesized SeNPs could be effective in destroying the Gram-positive bacteria such as *Arthrobacter* sp. W1, which was also considered to have the excellent antibacterial activity. Singh et al. (2015) reported that the biosynthetic SeNPs showed good antibacterial activity against *Bacillus* sp., but not against *E. coli* (Singh et al. 2015). This result tallied well with ours.

Conclusion

A facile one-pot and effective green process for biogenic SeNPs was obtained using the yeast *Magnusiomyces ingens* LH-F1 cell-free extracts for the first time. In the present study, SeO_2 2 mM, protein 500 mg L^{-1} and pH 7 were preferable to the biosynthesis of SeNPs, and the effects of pH, SeO_2 concentration and protein concentration on the synthesis process were different. The diameter of spherical and quasi-spherical SeNPs was mainly distributed in 70–90 nm (the average particles size was 87.82 ± 2.71 nm). The synthesized SeNPs were composed of standard hexagonal crystalline Se with high purity. Some biomolecules could play significant roles in SeNPs synthesis, which probably acted as reducing agents and capping agents. This research provides a novel path to identify the specific protein responsible for nanoparticles biosynthesis in potential yeast. Furthermore, the SeNPs exhibited an obvious antibacterial activity to *Arthrobacter* sp. W1, which provided reference for antimicrobial application of biogenic SeNPs.

Acknowledgements The authors wish to acknowledge the Open Project of State Key Laboratory of Urban Water Resource and Environment, Harbin Institute of Technology (Grant No. ESK201529), and the National Natural Science Foundation of China (Grant No. 31800091) for providing financial support.

Compliance with ethical standards

Conflict of interest On behalf of all authors, the corresponding author states that there is no conflict of interest.

References

Ahmed KBA, Kalla D, Uppuluri KB et al (2014) Green synthesis of silver and gold nanoparticles employing levan, a biopolymer from *Acetobacter xylinum* NCIM 2526, as a reducing agent and capping agent. Carbohydr Polym 112:539–545. https://doi.org/10.1016/j.carbpol.2014.06.033

Butler CS, Debieux CM, Dridge EJ et al (2012) Biomineralization of selenium by the selenate-respiring bacterium *Thauera selenatis*. Biochem Soc Trans 40:1239–1243. https://doi.org/10.1042/BST20120087

Chaudhary S, Umar A, Mehta SK (2014) Surface functionalized selenium nanoparticles for biomedical applications. J Biomed Nanotechnol 10:3004–3042. https://doi.org/10.1166/jbn.2014.1985

Che L, Dong Y, Wu M et al (2017) Characterization of Selenite Reduction by *Lysinibacillus* sp. ZYM-1 and photocatalytic performance of biogenic selenium nanospheres. ACS Sustain Chem Eng 5:2535–2543. https://doi.org/10.1021/acssuschemeng.6b02889

Das SK, Liang J, Schmidt M et al (2012) Biomineralization mechanism of gold by zygomycete fungi *rhizopous oryzae*. ACS Nano 6:6165–6173. https://doi.org/10.1021/nn301502s

Debieux CM, Dridge EJ, Mueller CM et al (2011) A bacterial process for selenium nanosphere assembly. Proc Natl Acad Sci 108:13480–13485. https://doi.org/10.1073/pnas.1105959108

Dobias J, Suvorova EI, Bernier-Latmani R (2011) Role of proteins in controlling selenium nanoparticle size. Nanotechnology. https://doi.org/10.1088/0957-4484/22/19/195605

Dykman L, Khlebtsov N (2012) Gold nanoparticles in biomedical applications: recent advances and perspectives to biological and medical. Chem Soc Rev 41:2256–2282. https://doi.org/10.1039/c1cs15166e

Eswayah AS, Smith TJ, Gardiner PHE (2016) Microbial transformations of selenium species of relevance to bioremediation. Appl Environ Microbiol 82:4848–4859. https://doi.org/10.1128/AEM.00877-16

Fernández-Llamosas H, Castro L, Blázquez ML et al (2016) Biosynthesis of selenium nanoparticles by *Azoarcus* sp. CIB. Microb Cell Fact 15:1–10. https://doi.org/10.1186/s12934-016-0510-y

Gates B, Mayers B, Cattle B et al (2002) Synthesis and characterization of uniform nanowires of trigonal selenium. Adv Funct Mater 12:219–227. https://doi.org/10.1002/1616-3028(200203)12:3%3c219:AID-ADFM219%3e3.0.CO;2-U

Gore F, Fawell J, Bartram J (2010) Too much or too little? A review of the conundrum of selenium. J Water Health 8:405–416. https://doi.org/10.2166/wh.2009.060

Jayaramudu T, Raghavendra GM, Varaprasad K et al (2013) Iota-Carrageenan-based biodegradable Ag^0 nanocomposite hydrogels for

the inactivation of bacteria. Carbohydr Polym 95:188–194. https://doi.org/10.1016/j.carbpol.2013.02.075

Jayaramudu T, Varaprasad K, Raghavendra GM et al (2017) Green synthesis of tea Ag nanocomposite hydrogels via mint leaf extraction for effective antibacterial activity. J Biomater Sci Polym Ed 28:1588–1602. https://doi.org/10.1080/09205063.2017.1338501

Khiralla GM, El-Deeb BA (2015) Antimicrobial and antibiofilm effects of selenium nanoparticles on some foodborne pathogens. LWT Food Sci Technol 63:1001–1007. https://doi.org/10.1016/j.lwt.2015.03.086

Kumar S, Tomar MS, Acharya A (2015) Carboxylic group-induced synthesis and characterization of selenium nanoparticles and its anti-tumor potential on Dalton's lymphoma cells. Coll Surf B Biointerfaces 126:546–552. https://doi.org/10.1016/j.colsurfb.2015.01.009

Kumar N, Krishnani KK, Singh NP (2018) Comparative study of selenium and selenium nanoparticles with reference to acute toxicity, biochemical attributes, and histopathological response in fish. Environ Sci Pollut Res 25(9):8914–8927. https://doi.org/10.1007/s11356-017-1165-x

Laemmli UK (1970) Cleavage of structural proteins during the assembly of the head of bacteriophage T4. Nature 227:680–685. https://doi.org/10.1038/227680a0

Lampis S, Zonaro E, Bertolini C et al (2017) Selenite biotransformation and detoxification by *Stenotrophomonas maltophilia* SeITE02: novel clues on the route to bacterial biogenesis of selenium nanoparticles. J Hazard Mater 324:3–14. https://doi.org/10.1016/j.jhazmat.2016.02.035

Lin ZH, Wang CRC (2005) Evidence on the size-dependent absorption spectral evolution of selenium nanoparticles. Mater Chem Phys 92:591–594. https://doi.org/10.1016/j.matchemphys.2005.02.023

Malhotra A, Dolma K, Kaur N et al (2013) Biosynthesis of gold and silver nanoparticles using a novel marine strain of *Stenotrophomonas*. Bioresour Technol 142:727–731. https://doi.org/10.1016/j.biortech.2013.05.109

Mishra A, Tripathy SK, Wahab R et al (2011) Microbial synthesis of gold nanoparticles using the fungus *Penicillium brevicompactum* and their cytotoxic effects against mouse mayo blast cancer C_2C_{12} cells. Appl Microbiol Biotechnol 92:617–630. https://doi.org/10.1007/s00253-011-3556-0

Moghaddam AB, Namvar F, Moniri M et al (2015) Nanoparticles biosynthesized by fungi and yeast: a review of their preparation, properties, and medical applications. Molecules 20:16540–16565. https://doi.org/10.3390/molecules200916540

Park TJ, Lee KG, Lee SY (2016) Advances in microbial biosynthesis of metal nanoparticles. Appl Microbiol Biotechnol 100:521–534. https://doi.org/10.1007/s00253-015-6904-7

Qu Y, You S, Zhang X et al (2018) Biosynthesis of gold nanoparticles using cell-free extracts of *Magnusiomyces ingens* LH-F1 for nitrophenols reduction. Bioprocess Biosyst Eng 41:359–367. https://doi.org/10.1007/s00449-017-1869-9

Raghavendra GM, Jayaramudu T, Varaprasad K et al (2013) Cellulose-polymer-Ag nanocomposite fibers for antibacterial fabrics/skin scaffolds. Carbohydr Polym 93:553–560. https://doi.org/10.1016/j.carbpol.2012.12.035

Schröfel A, Kratošová G, Šafařík I et al (2014) Applications of biosynthesized metallic nanoparticles—a review. Acta Biomater 10:4023–4042. https://doi.org/10.1016/j.actbio.2014.05.022

Shakibaie M, Khorramizadeh MR, Faramarzi MA et al (2010) Biosynthesis and recovery of selenium nanoparticles and the effects on matrix metalloproteinase-2 expression. Biotechnol Appl Biochem 56:7–15. https://doi.org/10.1042/BA20100042

Shen W, Qu Y, Pei X et al (2017) Catalytic reduction of 4-nitrophenol using gold nanoparticles biosynthesized by cell-free extracts of *Aspergillus* sp. WL-Au. J Hazard Mater 321:299–306. https://doi.org/10.1016/j.jhazmat.2016.07.051

Singh N, Saha P, Rajkumar K et al (2015) Biogenic strain of silver and selenium nanoparticles by *Pseudomonas fluorescens* and *Cladosporium* sp. JAPSK3 isolated from coal mine samples and their antimicrobial activity. Int J Nanosci 14:1550017. https://doi.org/10.1142/S0219581X15500179

Singh P, Kim YJ, Zhang D et al (2016) Biological synthesis of nanoparticles from plants and microorganisms. Trends Biotechnol 34:588–599. https://doi.org/10.1016/j.tibtech.2016.02.006

Sonkusre P, Singh Cameotra S (2015) Biogenic selenium nanoparticles inhibit *Staphylococcus aureus* adherence on different surfaces. Coll Surf B Biointerfaces 136:1051–1057. https://doi.org/10.1016/j.colsurfb.2015.10.052

Srivastava N, Mukhopadhyay M (2013) Biosynthesis and structural characterization of selenium nanoparticles mediated by *Zooglea ramigera*. Powder Technol 244:26–29. https://doi.org/10.1016/j.powtec.2013.03.050

Stranges S, Marshall JR, Trevisan M et al (2006) Effects of selenium supplementation on cardiovascular disease incidence and mortality: secondary analyses in a randomized clinical trial. Am J Epidemiol 163:694–699. https://doi.org/10.1093/aje/kwj097

Tan L, Li H, Ning S et al (2014) Aerobic decolorization and degradation of azo dyes by suspended growing cells and immobilized cells of a newly isolated yeast *Magnusiomyces ingens* LH-F1. Bioresour Technol 158:321–328. https://doi.org/10.1016/j.biortech.2014.02.063

Tugarova AV, Kamnev AA (2017) Proteins in microbial synthesis of selenium nanoparticles. Talanta 174:539–547. https://doi.org/10.1016/j.talanta.2017.06.013

Tugarova AV, Mamchenkova PV, Dyatlova YA et al (2018) FTIR and Raman spectroscopic studies of selenium nanoparticles synthesised by the bacterium *Azospirillum thiophilum*. Spectrochim Acta Part A Mol Biomol Spectrosc 192:458–463. https://doi.org/10.1016/j.saa.2017.11.050

Vera P, Echegoyen Y, Canellas E et al (2016) Nano selenium as antioxidant agent in a multilayer food packaging material. Anal Bioanal Chem 408:6659–6670. https://doi.org/10.1007/s00216-016-9780-9

Vogel M, Fischer S, Maffert A et al (2018) Biotransformation and detoxification of selenite by microbial biogenesis of selenium-sulfur nanoparticles. J Hazard Mater 344:749–757. https://doi.org/10.1016/j.jhazmat.2017.10.034

Wadhwani SA, Shedbalkar UU, Singh R et al (2016) Biogenic selenium nanoparticles: current status and future prospects. Appl Microbiol Biotechnol 100:2555–2566. https://doi.org/10.1007/s00253-016-7300-7

Xia X, Wu S, Li N et al (2018) Novel bacterial selenite reductase CsrF responsible for Se(IV) and Cr(VI) reduction that produces nanoparticles in *Alishewanella* sp. WH16-1. J Hazard Mater 342:499–509. https://doi.org/10.1016/j.jhazmat.2017.08.051

Zhang J, Zhang SY, Xu JJ et al (2004) A new method for the synthesis of selenium nanoparticles and the application to construction of H_2O_2 biosensor. Chin Chem Lett 15:1345–1348

Zhang Y, Wang J, Zhang L (2010) Creation of highly stable selenium nanoparticles capped with hyperbranched polysaccharide in water. Langmuir 26:17617–17623. https://doi.org/10.1021/la1033959

Zhang X, Qu Y, Shen W et al (2016) Biogenic synthesis of gold nanoparticles by yeast *Magnusiomyces ingens* LH-F1 for catalytic reduction of nitrophenols. Coll Surf A Physicochem Eng Asp 497:280–285. https://doi.org/10.1016/j.colsurfa.2016.02.033